5441

NUWC-NPT Technical Memorandum 980169

Copy 1

Naval Undersea Warfare Center Division
Newport, Rhode Island

RANDOM SHADING AND PHASING EFFECTS ON THE BEAM PATTERN FOR SINGLE LINE AND TWIN LINE ARRAYS

Berhane Adal
Norman L. Owsley
Submarine Sonar Department

28 October 1998

Report Documentation Page

Form Approved
OMB No. 0704-0188

1. REPORT DATE	2. REPORT TYPE	3. DATES COVERED
28 OCT 1998	**Technical Memo**	**28-10-1998 to 28-10-1998**

4. TITLE AND SUBTITLE
Random Shading and Phasing Effects on the Beam Pattern for Single Line and Twin Line Arrays

5a. CONTRACT NUMBER

5b. GRANT NUMBER

5c. PROGRAM ELEMENT NUMBER

6. AUTHOR(S)
Berhane Adal; Norman Owsley

5d. PROJECT NUMBER
A600068

5e. TASK NUMBER

5f. WORK UNIT NUMBER

7. PERFORMING ORGANIZATION NAME(S) AND ADDRESS(ES)
Naval Undersea Warfare Center Division,1176 Howell Street,Newport,RI,02841

8. PERFORMING ORGANIZATION REPORT NUMBER

9. SPONSORING/MONITORING AGENCY NAME(S) AND ADDRESS(ES)
Office of Naval Research, Tactical Passive Active Towed Volumetric Arrays

10. SPONSOR/MONITOR'S ACRONYM(S)
ONR TPATVA

11. SPONSOR/MONITOR'S REPORT NUMBER(S)

12. DISTRIBUTION/AVAILABILITY STATEMENT
Approved for public release; distribution unlimited

13. SUPPLEMENTARY NOTES
NUWC2015

14. ABSTRACT
This technical memorandum describes the effects of amplitude and phase perturbations on the peak and average sidelobe levels of beam patterns obtained from single line and twin line towed linear arrays.

15. SUBJECT TERMS
sidelobe; beam patterns; towed arrays

16. SECURITY CLASSIFICATION OF:			17. LIMITATION OF ABSTRACT	18. NUMBER OF PAGES	19a. NAME OF RESPONSIBLE PERSON
a. REPORT	b. ABSTRACT	c. THIS PAGE			
unclassified	**unclassified**	**unclassified**	**Same as Report (SAR)**	**33**	

ABSTRACT

This technical memorandum describes the effects of amplitude and phase perturbations on the peak and average sidelobe levels of beam patterns obtained from single line and twin line towed linear arrays.

ADMINISTRATIVE INFORMATION

The work documented in this report was sponsored by the Office of Naval Research (ONR321ss) under the Tactical Passive Active Towed Volumetric Arrays (TPATVA), Project No. A600068. The principal investigators and authors of this report are Berhane Adal and Norman Owsley of the Naval Undersea Warfare Center Division Newport, Submarine Sonar Department, Code 2123.

TABLE OF CONTENTS

LIST OF ILLUSTRATIONS

LIST OF ILLUSTRATIONS (Cont'd)

LIST OF TABLES

LIST OF ABBREVIATIONS, ACRONYMS, AND SYMBOLS

3D	three-dimensional
a	probability function spread parameter
AZ	azimuth
b	amplitude beam pattern
BLAC	Blackman shading
c	speed of sound in water
d	transmitter spacing
D/E	depression/elevation
d_x	transmitter spacing in the x-axis
d_y	transmitter spacing in the y-axis
f	frequency
HAMM	Hamming shading
HANN	Hanning shading
MRA	maximum response axis
N	number of hydrophones (sensors)
p	probability function spread parameter
RECT	rectangular shading
SLL	sidelobe level
SLTA	single line towed array
TLTA	twin line towed array
TRIA	triangular shading
δ_n	random amplitude error
ε_n	random phase error
λ	wavelength of the signal
ω_n	error-free shading coefficient
ω'_n	shading coefficient
θ	direction of arrival angle

RANDOM SHADING AND PHASING EFFECTS ON THE BEAM PATTERN FOR SINGLE LINE AND TWIN LINE ARRAYS

1. INTRODUCTION

The hydrophone array is the critical device used under water to sense the direction pressure field properties of sound waves over a spatial aperture. The response of the hydrophone array varies with direction relative to the array. This variation with direction for a given array steering direction specifies the beam pattern of the array. A beam pattern is formed as a weighted (shaded) sum of each array element output. Similarly, a transmitting array radiation beam pattern can be formed by collecting individual acoustic source outputs. For any beam pattern case, amplitude shading is a convenient way to tailor the beam pattern to a desired shape. However, due to various amplitude and phase perturbations in either the hydrophone or the transmission channel, the beam pattern will have imperfections when compared to the desired beam pattern shape.

In this study, imperfections affecting the amplitude and phase of the desired beam pattern are modeled by random shading and phasing. In the presence of noisy environments (e.g., channel noise, interfering plane waves) which interfere at angles outside the mainlobe of the beam pattern, it is often desirable to reduce the sidelobe levels. Relative reductions achieved with a rectangular (RECT) window function are used in this study as a baseline. Common practice is to select an aperture amplitude/phase shading function that reduces the sidelobes to an acceptable peak with minimal mainlobe spreading. Results obtained using triangular (TRIA), Hanning (HANN), Blackman (BLAC), and Hamming (HAMM) window functions are compared to results obtained using RECT shading. Effects of random shading and phasing on the peak and average sidelobe levels (SLLs) of the beam patterns are then shown using simulations. Simulations are performed using a single line towed array (SLTA) and a twin line towed array (TLTA).

2. SINGLE LINE TOWED ARRAY

Consider the angular response of a linear hydrophone array to a plane wave signal as a function of the direction of arrival. Suppose the linear hydrophone array is aligned with the x-axis so that θ is the angle between the direction of arrival and the x-axis (see figure 1). With this choice, the signal received at any point in the array is a function only of θ. The amplitude beam pattern of a linear array of N sensors for a beam with a maximum response axis (MRA) θ_j and an incident single frequency plane wave with frequency f and direction of arrival angle θ may be written as

$$b(\theta, f) = \left| \sum_{n=1}^{N} \omega_n' e^{-i\frac{2\pi}{\lambda} d(\cos\theta - \cos\theta_j)(n-1)} \right|^2, \quad (1)$$

where $\lambda = c/f = \dfrac{1500\, m/s}{f}$ is the wavelength of the signal,

ω_n' is the actual shading coefficient at the n^{th} element of the array, and

c is the speed of sound in the water.

The shading coefficient ω_n' is related to the error-free shading coefficient ω_n by

$$\omega_n' = \omega_n (1 + \delta_n) e^{i\varepsilon_n}, \quad (2)$$

where δ_n and ε_n are the random amplitude and phase errors, respectively. The shading coefficients for an $N = 16$ SLTA are presented in table 1. Figure 2 illustrates the peak and average SLLs for the single line array.

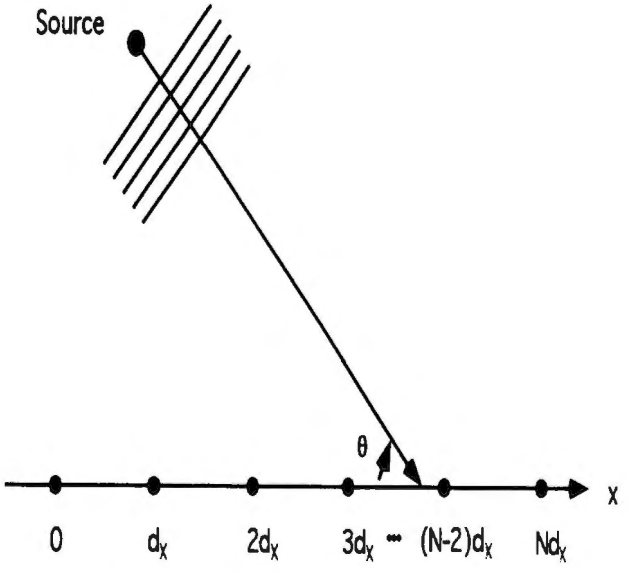

Figure 1. Single Line Array Geometry and Bearing Coordinate System

Table 1. Shading Coefficients for N = 16 Single Line Towed Array (SLTA)

RECT		TRIA		HANN		BLAC		HAMM	
ω_n'	dB	ω_n'	dB	ω_n'	dB	ω_n'	dB	ω_n'	dB
1.00	0.00	0.12	-18.59	0.03	-29.43	0.01	-37.80	0.11	-19.09
1.00	0.00	0.24	-12.57	0.13	-17.69	0.06	-24.75	0.20	-13.98
1.00	0.00	0.35	-9.05	0.28	-11.15	0.15	-16.54	0.33	-9.50
1.00	0.00	0.47	-6.55	0.45	-6.86	0.30	-10.60	0.50	-6.06
1.00	0.00	0.59	-4.61	0.64	-3.92	0.49	-6.22	0.67	-3.53
1.00	0.00	0.71	-3.03	0.80	-1.92	0.70	-3.11	0.82	-1.75
1.00	0.00	0.82	-1.69	0.93	-0.68	0.88	-1.10	0.93	-0.62
1.00	0.00	0.94	-0.53	0.99	-0.07	0.99	-0.12	0.99	-0.07
1.00	0.00	0.94	-0.53	0.99	-0.07	0.99	-0.12	0.99	-0.07
1.00	0.00	0.82	-1.69	0.93	-0.68	0.88	-1.10	0.93	-0.62
1.00	0.00	0.71	-3.03	0.80	-1.92	0.70	-3.11	0.82	-1.75
1.00	0.00	0.59	-4.61	0.64	-3.92	0.49	-6.22	0.67	-3.53
1.00	0.00	0.47	-6.55	0.45	-6.86	0.30	-10.60	0.50	-6.06
1.00	0.00	0.35	-9.05	0.28	-11.15	0.15	-16.54	0.33	-9.50
1.00	0.00	0.24	-12.57	0.13	-17.69	0.06	-24.75	0.20	-13.98
1.00	0.00	0.12	-18.59	0.03	-29.43	0.01	-37.80	0.11	-19.09

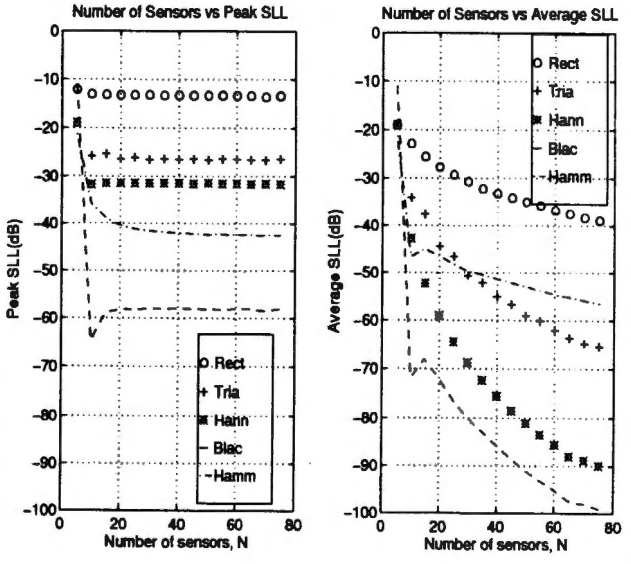

Figure 2. Peak and Average SLL versus Single Line Towed Array Size

3. TWIN LINE TOWED ARRAY

Consider an array geometry as shown in figure 3. Let the sensor element spacing in the x- and y-directions be d_x and d_y, respectively. Then, the coordinates for the mn^{th} hydrophone element are $x_m = md_x$, $y_n = nd_y$, and $z_{m,n} = 0$. The amplitude beam pattern steered in the azimuthal (AZ_o) and depression/elevation (DE_o) angles of the MRA of a twin line array arranged in the xy plane with spacing d_x and d_y between elements may be written as

$$b(AZ, DE, f) = \left| \sum_{m=1}^{N_x} \sum_{n=1}^{N_y} \omega'_{mn} e^{-i\frac{2\pi}{\lambda}\left(md_x\left[\cos(DE)\sin(AZ)-\cos(DE_o)\sin(AZ_o)\right]+nd_y\left[\cos(DE)\cos(AZ)-\cos(DE_o)\cos(AZ_o)\right]\right)} \right|^2, \tag{3}$$

where $\lambda = c/f = \dfrac{1500\, m/s}{f}$ is the signal wavelength, and

ω'_{mn} is the actual shading coefficient at the mn^{th} element of the array.

The shading coefficient ω'_{mn} is related to the error-free shading coefficient ω_{mn} by

$$\omega'_{mn} = \omega_{mn}\left(1+\delta_{mn}\right)e^{i\varepsilon_{mn}}, \tag{4}$$

where δ_{mn} and ε_{mn} are the random amplitude and phase errors, respectively.

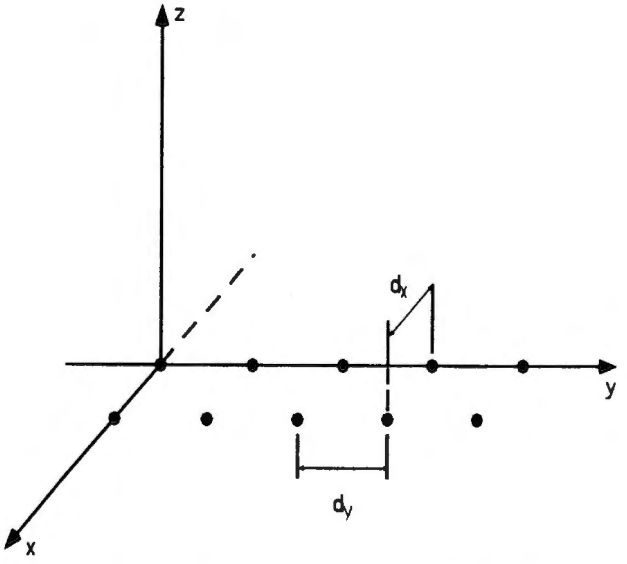

Figure 3. Twin Line Array Geometry and Bearing Coordinate System

As an example, consider the beam pattern for a 15 x 2 line array using error-free RECT shading at frequency f = 850 Hz (see figure 4). Element spacing in the x- and y-directions is 0.4424 m and 0.69 m, respectively. The elements are phased to steer the main beam maximum response at 90° azimuth and 0° D/E. The peak SLL is -13.4 dB and the peak backlobe level at 270° is approximately -47 dB.

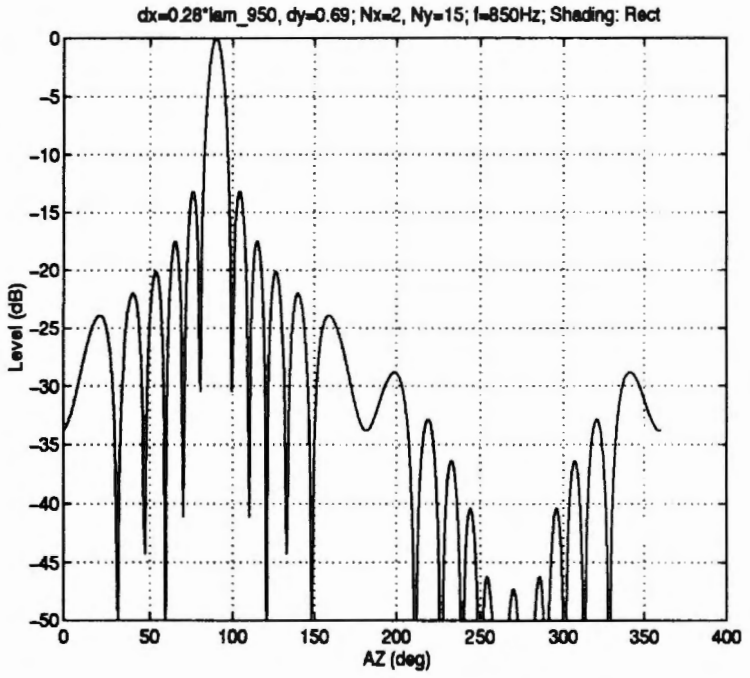

Figure 4. Twin Line Array Beam Pattern at AZ_o = 90° and DE_o = 0°

Other error-free shadings were used to study the effects on the peak and average SLLs, as well as on the peak backlobe levels. Figures 5, 6a, 6b, and 6c depict the beam patterns of a twin line array consisting of identical lines of equally spaced elements. The beams were obtained using equation (3) in the look direction of DE_O = 0° and AZ_O = 90°. Figure 5 illustrates an N = 30 twin line array at f = 850 Hz, and figures 6a, 6b, and 6c illustrate an N = 62 twin line array at frequencies 750, 850, and 950 Hz, respectively. The beams are shaded with error-free shading coefficients. The peak SLLs corresponding to the five shading methods decreased from -13.4 dB (RECT) to less than -50 dB (HAMM). The effect of the three frequencies used can be observed from the peak backlobe level at 270° (see figures 6a - 6c). Figures 6a through 6c also illustrate that the backlobe can be controlled using a twin line array of identical and equally spaced transmitters. Furthermore, a matrix projection operator can be used to produce a broadband null on the backlobe of the quiescent beam pattern with insignificant perturbation of the pattern remote from the null.

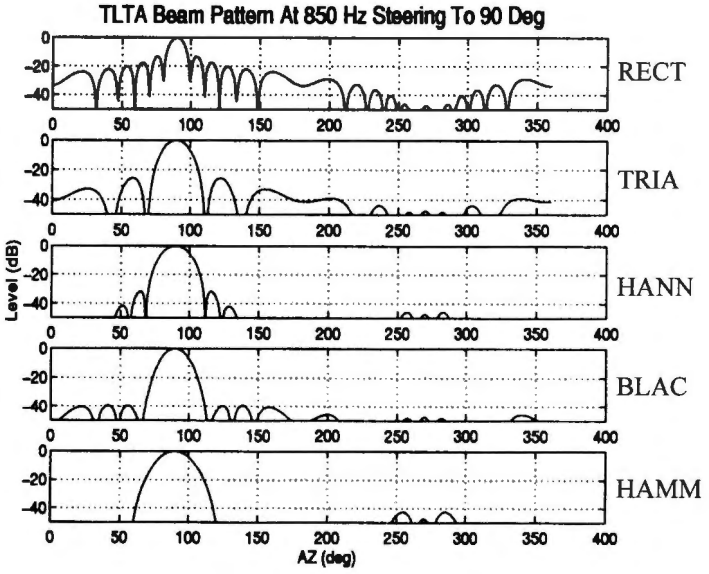

Figure 5. Beam Pattern Shading for N = 30, f = 850 Hz TLTA

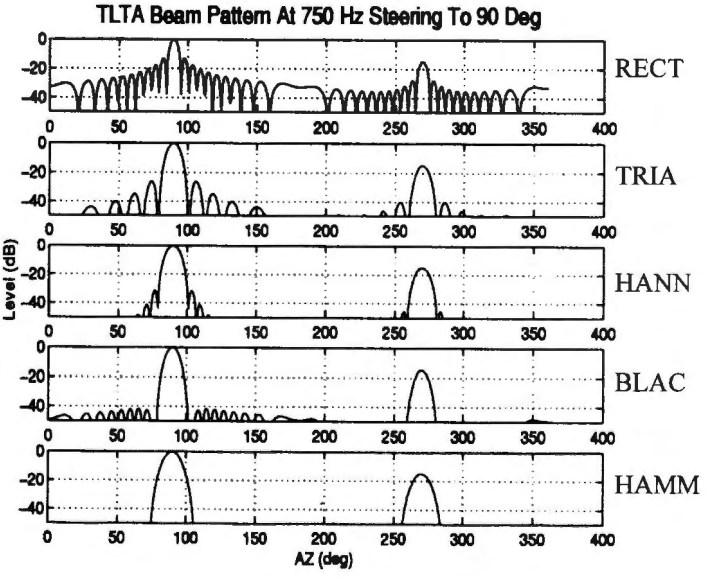

Figure 6a. Beam Pattern Shading for N = 62, f = 750 Hz TLTA

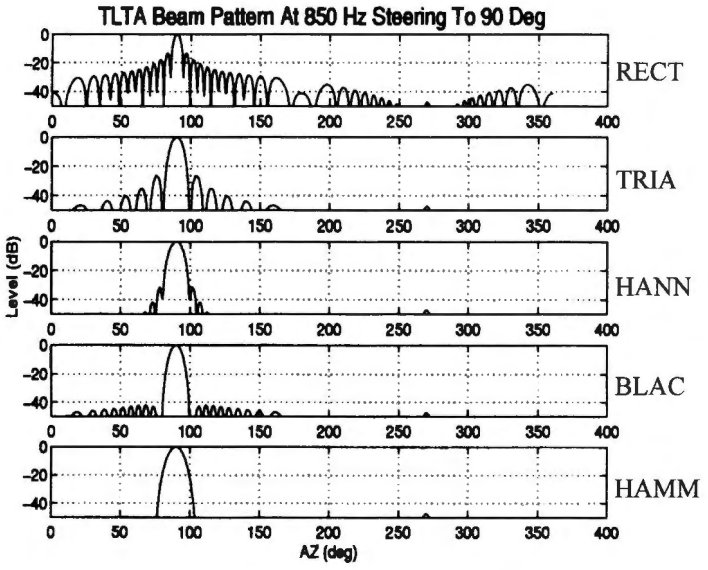

Figure 6b. Beam Pattern Shading for N = 62, f = 850 Hz TLTA

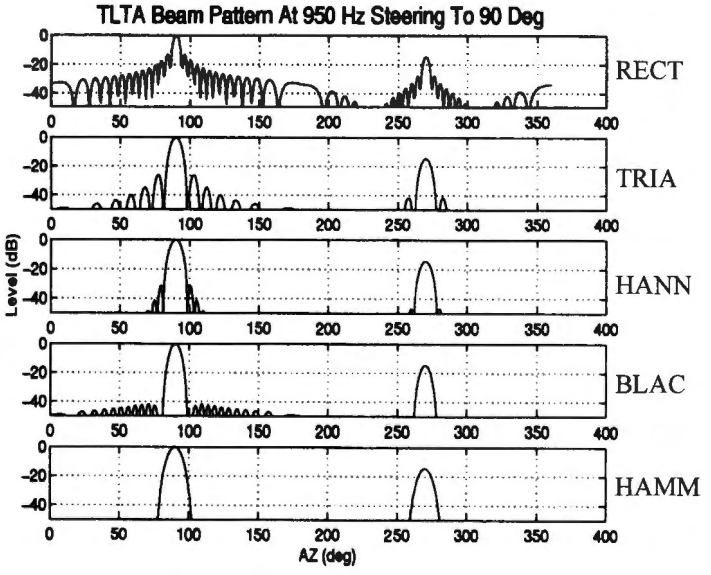

Figure 6c. Beam Pattern Shading for N = 62, f = 950 Hz TLTA

4. SIMULATION RESULTS

The simulation results for both SLTA and TLTA are grouped according to the number of array elements and the frequencies used. Array elements selected were $N = 16$, 32, and 64 for the SLTA and $N = 30$ and 62 for the TLTA. Element spacing of $d = 0.69$ m was used for the SLTA. Element spacing $d_x = 0.4424$ m and $d_y = 0.69$ m was used for the TLTA. The shading and phasing were perturbed using zero-mean, independent random variables uniformly distributed over [-0.1, 0.1] and [-10°, 10°], respectively. The range of randomness accounts for 20% of the maximum amplitude value of 1. The perturbation variance is 25 dB below the maximum amplitude. Simulation results were obtained by ensemble averaging 50 runs wherein statistically independent perturbations of amplitude alone, phase alone, and amplitude and phase together were generated.

4.1 SINGLE LINE TOWED ARRAY

Figures 7a through 9b show the peak and average SLLs of beam patterns obtained by perturbing the various shading coefficients in amplitude and phase. Random shading effects on the peak and average SLLs for the SLTA are shown in figures 7a, 8a, and 9a. Similarly, the effects of phase errors are shown in figures 7b, 8b, and 9b. Figures 7c, 7d, 8c, and 8d show the combined effects of simultaneous random amplitude and phase on peak and average SLLs. Amplitude shading and phasing effects were compared to the error-free shading and phasing by referring to the peak and average SLLs corresponding to $a = 0$ and $p = 0$. The figures show that increasing the uniform probability function spread parameters a and p raises the amplitude of the SLL. Generally, phase random errors seemed to have a greater effect on the SLLs than amplitude. This phase effect is easily observed on HANN, BLAC, and HAMM shading. Three cases are delineated for the single line towed array:

- Case 1a: $N = 16, f = 850$ Hz (shown in figures 7a through 7d)
- Case 1b: $N = 32, f = 850$ Hz (shown in figures 8a through 8d)
- Case 1c: $N = 64, f = 850$ Hz (shown in figures 9a and 9b)

Figures 7a and 7b depict a single line array with $N = 16, f = 850$ Hz (case 1a). Peak SLLs using RECT, TRIA, and HANN shading are shown to be the least sensitive to random shading and phasing effects. For average SLL, the least sensitive to phase perturbation is RECT shading; however, its peak SLL is high. In all the other shading schemes, the average SLL increased as the amplitude or phase errors were increased. As is apparent from these graphics, random shading effects on peak and average SLLs were less pronounced than random phasing effects. If only amplitude errors are considered, HANN shading is preferred over the other methods for being one of the least sensitive and having low (about -30 dB) peak SLL. However, TRIA shading is the best choice if both amplitude and phase effects are considered.

Figures 7c and 7d are three-dimensional (3D) to show the combined amplitude and phase perturbation effects on the sidelobe levels. The peak and average SLLs increased as a result of increasing both amplitude and phase errors.

Case 1a considers the SLTA for $N = 16, f = 850$ Hz (figures 7a through 7d).

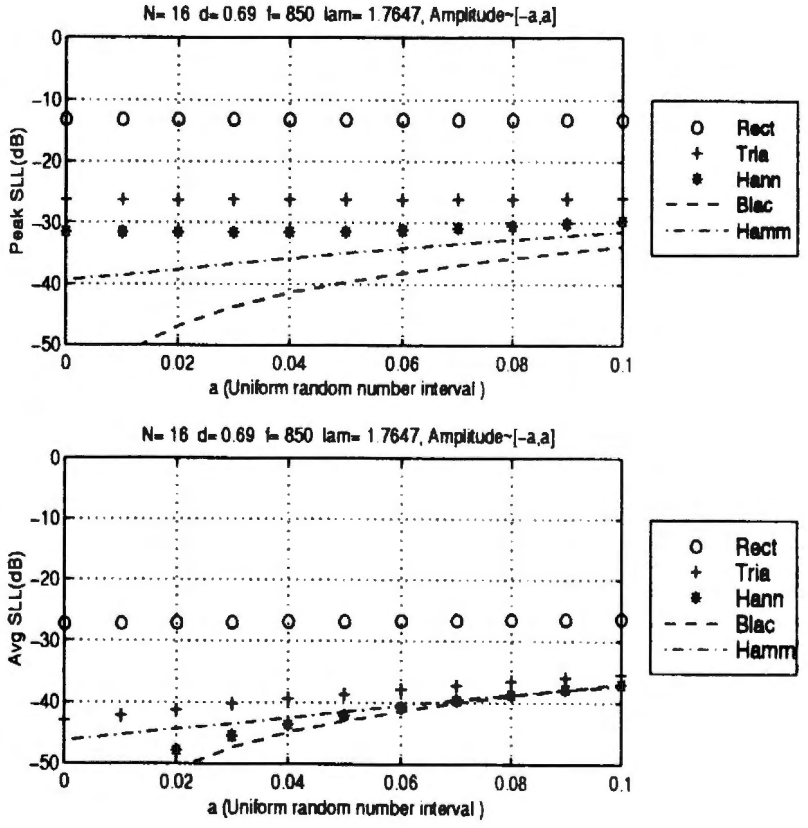

Figure 7a. Random Shading Effects on the Peak and Average SLL of Beam Patterns for N = 16, f = 850 Hz SLTA

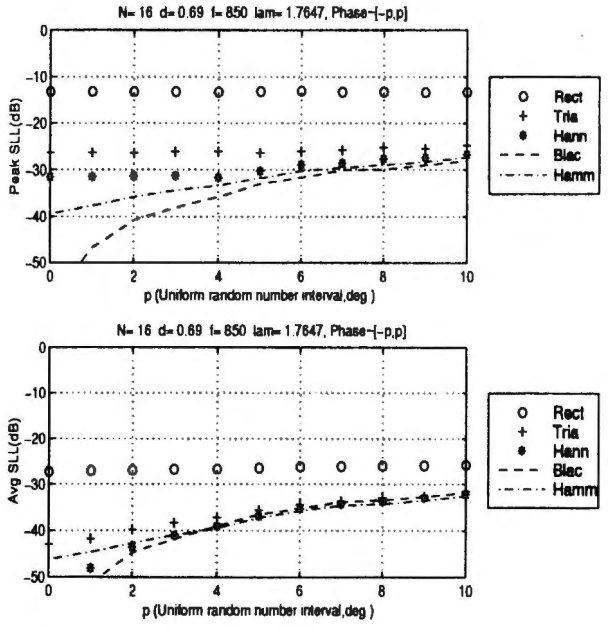

Figure 7b. Random Phasing Effects on the Peak and Average SLL of Beam Patterns for N = 16, f = 850 Hz SLTA

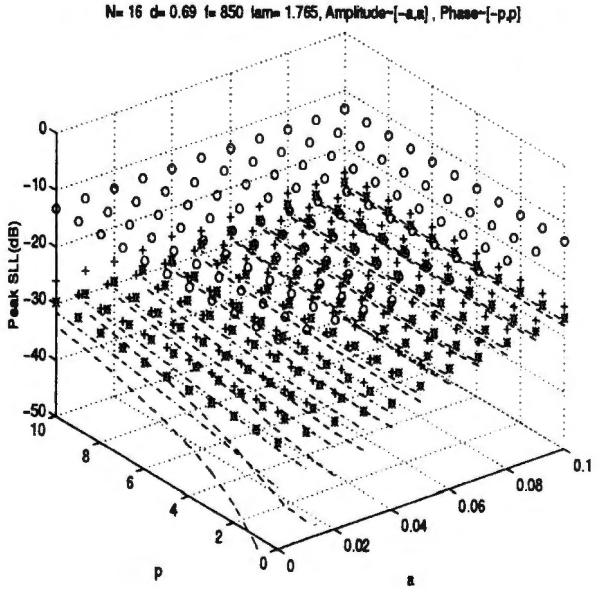

Figure 7c. Random Shading and Phasing Error Effects on the Peak SLL of Beam Patterns for N = 16, f = 850 Hz SLTA

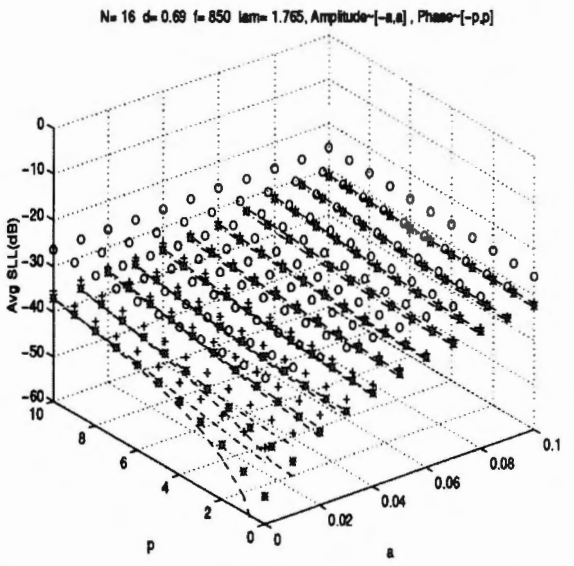

Figure 7d. Random Shading and Phasing Error Effects on the Average SLL of Beam Patterns for $N = 16$, $f = 850$ Hz SLTA

The simulations were repeated using the larger array sizes, $N = 32$ (case 1b) and $N = 64$ (case 1c). Figures 8a through 8d depict case 1b. Figures 9a and 9b illustrate case 1c. The effects of a larger array size, as well as shading and phasing errors, were observed. Larger array sizes produced lower average SLL beam patterns (see figure 2); however, the peak SLL of a larger array size was only slightly lower than that of a smaller array. Therefore, the effect of errors due to shading and phasing on the average SLLs would be expected to be less pronounced. This effect can be observed by comparing the results of the single line array of length $N = 16$ versus $N = 64$. The plots indicate that RECT, TRIA, and HANN are not very sensitive to amplitude shading. These indications are observed by the almost constant values of the three shading schemes. BLAC and HAMM shading are very sensitive to amplitude shading. For example, for $N = 16$, the peak deviations of BLAC and HAMM are about 25 and 8 dB, respectively. Cases of $N = 32$ and 64 also exhibit similar deviations. Table 2 lists the shading coefficients for an $N = 32$ SLTA. Table 3 lists the shading coefficients for an $N = 64$ SLTA.

Independent of the array size, the curves show that RECT shading is the least sensitive to phase perturbation. The peak and average SLLs of the beam pattern when using HANN, BLAC, and HAMM shading seem to converge to the same values. Aside from RECT shading, the peak and average SLLs seem to converge to the same values. Hence, the amplitude shading method with the largest error-free peak and average SLL deviations corresponds to the least sensitive to perturbation. Again, TRIA shading outperformed the other shading methods.

Case 1b considers the SLTA for $N = 32, f = 850$ Hz (figures 8a through 8d).

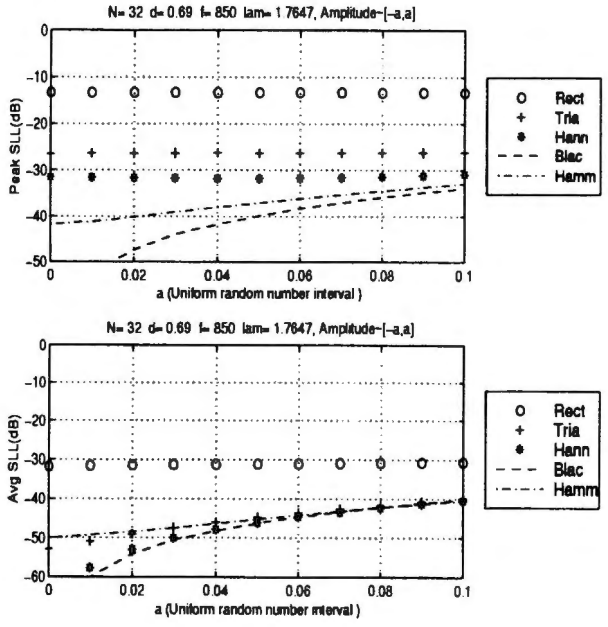

Figure 8a. Random Shading Effects on the Peak and Average SLL of Beam Patterns for N = 32, f = 850 Hz SLTA

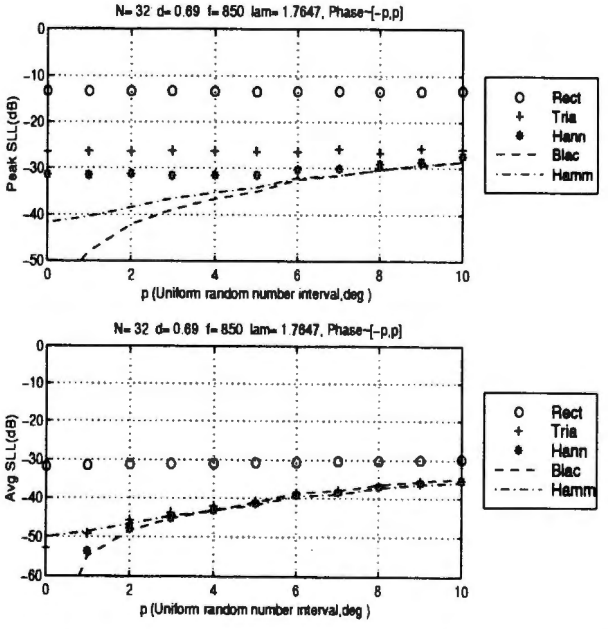

Figure 8b. Random Phasing Effects on the Peak and Average SLL of Beam Patterns for N = 32, f = 850 Hz SLTA

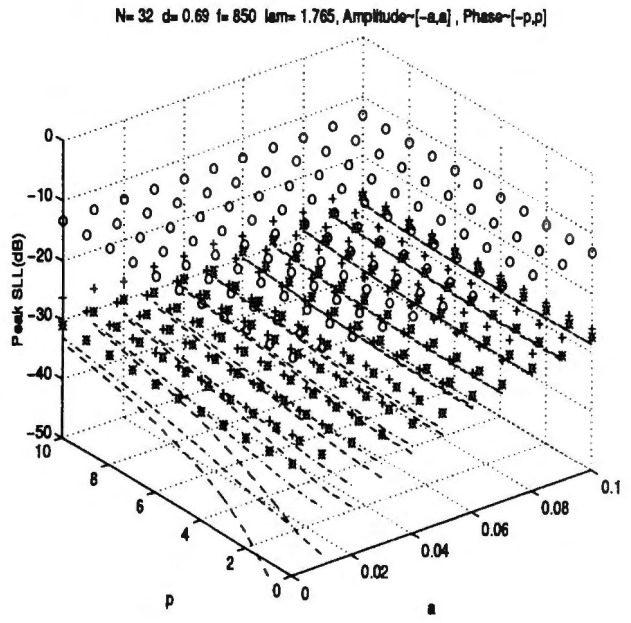

Figure 8c. Random Shading and Phasing Error Effects on the Peak SLL of Beam Patterns for N = 32, f = 850 Hz SLTA

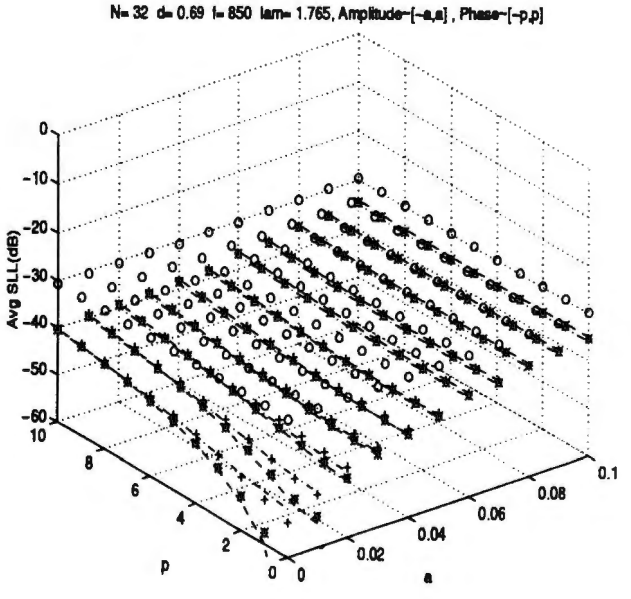

Figure 8d. Random Shading and Phasing Error Effects on the Average SLL of Beam Patterns for N = 32, f = 850 Hz SLTA

Case 1c considers the SLTA for $N = 64, f = 850$ Hz (figures 9a and 9b).

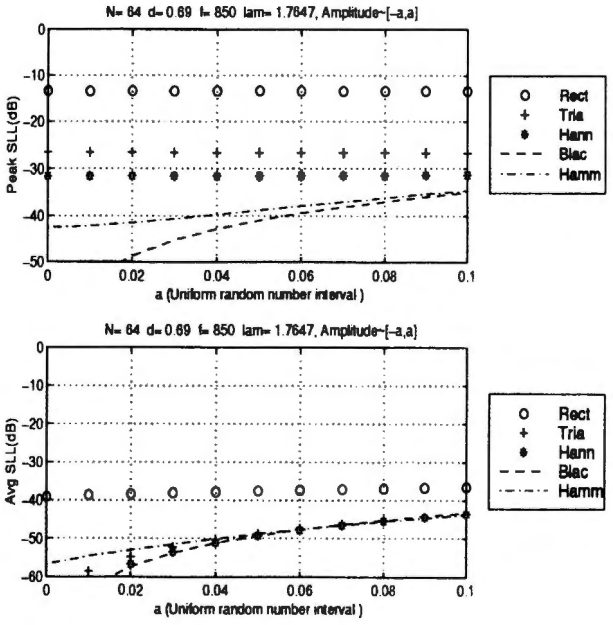

Figure 9a. Random Shading Effects on the Peak and Average SLL of Beam Patterns for N = 64, f = 850 Hz SLTA

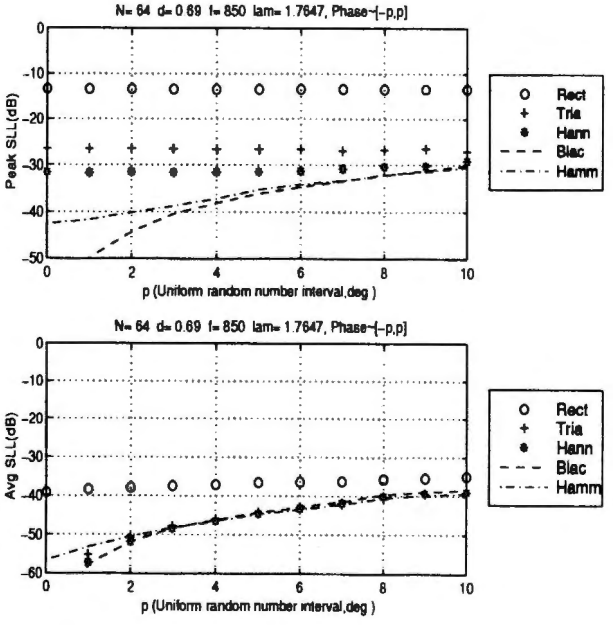

Figure 9b. Random Phasing Effects on the Peak and Average SLL of Beam Patterns for N = 64, f = 850 Hz SLTA

Table 2. Shading Coefficients for N = 32 SLTA

RECT		TRIA		HANN		BLAC		HAMM	
ω_n'	dB	ω_n'	dB	ω_n'	dB	ω_n'	dB	ω_n'	dB
1.00	0.00	0.06	-24.35	0.01	-40.88	0.00	-49.62	0.09	-21.08
1.00	0.00	0.12	-18.33	0.04	-28.92	0.01	-37.26	0.11	-18.94
1.00	0.00	0.18	-14.81	0.08	-22.01	0.03	-29.73	0.15	-16.30
1.00	0.00	0.24	-12.31	0.14	-17.19	0.06	-24.16	0.21	-13.68
1.00	0.00	0.30	-10.37	0.21	-13.56	0.10	-19.68	0.27	-11.27
1.00	0.00	0.36	-8.79	0.29	-10.68	0.16	-15.92	0.35	-9.15
1.00	0.00	0.42	-7.45	0.38	-8.36	0.23	-12.73	0.43	-7.30
1.00	0.00	0.48	-6.29	0.48	-6.44	0.32	-9.99	0.52	-5.71
1.00	0.00	0.55	-5.26	0.57	-4.86	0.41	-7.65	0.61	-4.36
1.00	0.00	0.61	-4.35	0.66	-3.56	0.52	-5.67	0.69	-3.22
1.00	0.00	0.67	-3.52	0.75	-2.50	0.63	-4.01	0.77	-2.27
1.00	0.00	0.73	-2.77	0.83	-1.65	0.74	-2.66	0.84	-1.50
1.00	0.00	0.79	-2.07	0.89	-0.98	0.83	-1.60	0.90	-0.90
1.00	0.00	0.85	-1.43	0.94	-0.50	0.91	-0.81	0.95	-0.46
1.00	0.00	0.91	-0.83	0.98	-0.18	0.97	-0.29	0.98	-0.16
1.00	0.00	0.97	-0.27	1.00	-0.02	1.00	-0.03	1.00	-0.02
1.00	0.00	0.97	-0.27	1.00	-0.02	1.00	-0.03	1.00	-0.02
1.00	0.00	0.91	-0.83	0.98	-0.18	0.97	-0.29	0.98	-0.16
1.00	0.00	0.85	-1.43	0.94	-0.50	0.91	-0.81	0.95	-0.46
1.00	0.00	0.79	-2.07	0.89	-0.98	0.83	-1.60	0.90	-0.90
1.00	0.00	0.73	-2.77	0.83	-1.65	0.74	-2.66	0.84	-1.50
1.00	0.00	0.67	-3.52	0.75	-2.50	0.63	-4.01	0.77	-2.27
1.00	0.00	0.61	-4.35	0.66	-3.56	0.52	-5.67	0.69	-3.22
1.00	0.00	0.55	-5.26	0.57	-4.86	0.41	-7.65	0.61	-4.36
1.00	0.00	0.48	-6.29	0.48	-6.44	0.32	-9.99	0.52	-5.71
1.00	0.00	0.42	-7.45	0.38	-8.36	0.23	-12.73	0.43	-7.30
1.00	0.00	0.36	-8.79	0.29	-10.68	0.16	-15.92	0.35	-9.15
1.00	0.00	0.30	-10.37	0.21	-13.56	0.10	-19.68	0.27	-11.27
1.00	0.00	0.24	-12.31	0.14	-17.19	0.06	-24.16	0.21	-13.68
1.00	0.00	0.18	-14.81	0.08	-22.01	0.03	-29.73	0.15	-16.30
1.00	0.00	0.12	-18.33	0.04	-28.92	0.01	-37.26	0.11	-18.94
1.00	0.00	0.06	-24.35	0.01	-40.88	0.00	-49.62	0.09	-21.08

Table 3. Shading Coefficients for N = 64 SLTA

RECT		TRIA		HANN		BLAC		HAMM	
ω_n'	dB	ω_n'	dB	ω_n'	dB	ω_n'	dB	ω_n'	dB
1.00	0.00	0.03	-30.24	0.00	-52.64	0.00	-61.48	0.08	-21.71
1.00	0.00	0.06	-24.22	0.01	-40.62	0.00	-49.35	0.09	-21.05
1.00	0.00	0.09	-20.70	0.02	-33.61	0.01	-42.16	0.10	-20.07
1.00	0.00	0.12	-18.20	0.04	-28.66	0.01	-36.98	0.11	-18.86
1.00	0.00	0.15	-16.26	0.06	-24.84	0.02	-32.87	0.13	-17.54
1.00	0.00	0.18	-14.67	0.08	-21.75	0.03	-29.44	0.16	-16.18
1.00	0.00	0.22	-13.34	0.11	-19.16	0.05	-26.48	0.18	-14.83
1.00	0.00	0.25	-12.18	0.14	-16.94	0.06	-23.86	0.21	-13.52
1.00	0.00	0.28	-11.15	0.18	-15.01	0.08	-21.50	0.24	-12.27
1.00	0.00	0.31	-10.24	0.22	-13.31	0.11	-19.36	0.28	-11.10
1.00	0.00	0.34	-9.41	0.26	-11.80	0.13	-17.41	0.32	-9.99
1.00	0.00	0.37	-8.65	0.30	-10.45	0.17	-15.61	0.36	-8.96
1.00	0.00	0.40	-7.96	0.35	-9.23	0.20	-13.95	0.40	-8.01
1.00	0.00	0.43	-7.32	0.39	-8.13	0.24	-12.41	0.44	-7.12
1.00	0.00	0.46	-6.72	0.44	-7.14	0.28	-10.99	0.48	-6.29
1.00	0.00	0.49	-6.16	0.49	-6.23	0.33	-9.68	0.53	-5.53
1.00	0.00	0.52	-5.63	0.54	-5.41	0.38	-8.47	0.57	-4.83
1.00	0.00	0.55	-5.13	0.58	-4.67	0.43	-7.36	0.62	-4.19
1.00	0.00	0.58	-4.66	0.63	-3.99	0.48	-6.33	0.66	-3.60
1.00	0.00	0.62	-4.22	0.68	-3.38	0.54	-5.39	0.70	-3.06
1.00	0.00	0.65	-3.79	0.72	-2.83	0.59	-4.54	0.74	-2.57
1.00	0.00	0.68	-3.39	0.76	-2.34	0.65	-3.76	0.78	-2.13
1.00	0.00	0.71	-3.00	0.80	-1.90	0.70	-3.07	0.82	-1.73
1.00	0.00	0.74	-2.63	0.84	-1.51	0.75	-2.44	0.85	-1.38
1.00	0.00	0.77	-2.28	0.87	-1.17	0.80	-1.90	0.88	-1.07
1.00	0.00	0.80	-1.94	0.90	-0.87	0.85	-1.42	0.91	-0.80
1.00	0.00	0.83	-1.61	0.93	-0.62	0.89	-1.01	0.94	-0.57
1.00	0.00	0.86	-1.29	0.95	-0.41	0.93	-0.68	0.96	-0.38
1.00	0.00	0.89	-0.99	0.97	-0.25	0.95	-0.41	0.97	-0.23
1.00	0.00	0.92	-0.70	0.99	-0.13	0.98	-0.21	0.99	-0.12
1.00	0.00	0.95	-0.41	0.99	-0.05	0.99	-0.07	1.00	-0.04
1.00	0.00	0.98	-0.13	1.00	-0.01	1.00	-0.01	1.00	0.00

Table 3. Shading Coefficients for N = 64 SLTA (Cont'd)

RECT		TRIA		HANN		BLAC		HAMM	
ω'_n	dB	ω'_n	dB	ω'_n	dB	ω'_n	dB	ω'_n	dB
1.00	0.00	0.98	-0.13	1.00	-0.01	1.00	-0.01	1.00	0.00
1.00	0.00	0.95	-0.41	0.99	-0.05	0.99	-0.07	1.00	-0.04
1.00	0.00	0.92	-0.70	0.99	-0.13	0.98	-0.21	0.99	-0.12
1.00	0.00	0.89	-0.99	0.97	-0.25	0.95	-0.41	0.97	-0.23
1.00	0.00	0.86	-1.29	0.95	-0.41	0.93	-0.68	0.96	-0.38
1.00	0.00	0.83	-1.61	0.93	-0.62	0.89	-1.01	0.94	-0.57
1.00	0.00	0.80	-1.94	0.90	-0.87	0.85	-1.42	0.91	-0.80
1.00	0.00	0.77	-2.28	0.87	-1.17	0.80	-1.90	0.88	-1.07
1.00	0.00	0.74	-2.63	0.84	-1.51	0.75	-2.44	0.85	-1.38
1.00	0.00	0.71	-3.00	0.80	-1.90	0.70	-3.07	0.82	-1.73
1.00	0.00	0.68	-3.39	0.76	-2.34	0.65	-3.76	0.78	-2.13
1.00	0.00	0.65	-3.79	0.72	-2.83	0.59	-4.54	0.74	-2.57
1.00	0.00	0.62	-4.22	0.68	-3.38	0.54	-5.39	0.70	-3.06
1.00	0.00	0.58	-4.66	0.63	-3.99	0.48	-6.33	0.66	-3.60
1.00	0.00	0.55	-5.13	0.58	-4.67	0.43	-7.36	0.62	-4.19
1.00	0.00	0.52	-5.63	0.54	-5.41	0.38	-8.47	0.57	-4.83
1.00	0.00	0.49	-6.16	0.49	-6.23	0.33	-9.68	0.53	-5.53
1.00	0.00	0.46	-6.72	0.44	-7.14	0.28	-10.99	0.48	-6.29
1.00	0.00	0.43	-7.32	0.39	-8.13	0.24	-12.41	0.44	-7.12
1.00	0.00	0.40	-7.96	0.35	-9.23	0.20	-13.95	0.40	-8.01
1.00	0.00	0.37	-8.65	0.30	-10.45	0.17	-15.61	0.36	-8.96
1.00	0.00	0.34	-9.41	0.26	-11.80	0.13	-17.41	0.32	-9.99
1.00	0.00	0.31	-10.24	0.22	-13.31	0.11	-19.36	0.28	-11.10
1.00	0.00	0.28	-11.15	0.18	-15.01	0.08	-21.50	0.24	-12.27
1.00	0.00	0.25	-12.18	0.14	-16.94	0.06	-23.86	0.21	-13.52
1.00	0.00	0.22	-13.34	0.11	-19.16	0.05	-26.48	0.18	-14.83
1.00	0.00	0.18	-14.67	0.08	-21.75	0.03	-29.44	0.16	-16.18
1.00	0.00	0.15	-16.26	0.06	-24.84	0.02	-32.87	0.13	-17.54
1.00	0.00	0.12	-18.20	0.04	-28.66	0.01	-36.98	0.11	-18.86
1.00	0.00	0.09	-20.70	0.02	-33.61	0.01	-42.16	0.10	-20.07
1.00	0.00	0.06	-24.22	0.01	-40.62	0.00	-49.35	0.09	-21.05
1.00	0.00	0.03	-30.24	0.00	-52.64	0.00	-61.48	0.08	-21.71

4.2 TWIN LINE TOWED ARRAY

As in the single line array case, shading coefficients perturbed in amplitude and phase were used to study the effects on the peak and average SLLs of various beam patterns of the twin line towed array (TLTA). These effects were also observed as a function of array size and frequency. Array lengths of $N = 16$, 32, and 64 were used in the single line array simulations. The sizes used in the twin line array simulations were $N = 30$ and 62. Comparisons of array length $N = 32$ and 64 of the single line array were made against $N = 30$ and 62 of the twin line array, respectively. Cases 2a and 2b show the simulation study plots of the TLTA at various frequencies for $N = 30$ and $N = 62$, respectively. Case 2a is illustrated in figures 10a through 12b. Case 2b is depicted in figures 13a through 15b.

Figures 10a through 12b for the twin line array show results generally similar to those obtained using the single line array and nearly identical results at 850 Hz. The average SLL simulation results of the twin line array are as robust as the single line array case. The only difference is that all results except those using RECT shading (5 dB lower) were $\approx$ 5 dB higher than results for the single line array. At 750 and 950 Hz, twin line array simulation results were different than the various patterns (especially peak SLL) observed on both arrays at 850 Hz. These effects are due to the presence of backlobe with levels that are perturbation insensitive when using the twin line array. For RECT shading, the peak SLL (-13 dB) at about 105° (as in the single line array case) was larger than the peak backlobe level (-15 dB); hence, the peak SLL simulation results using RECT shading were unaffected by the backlobe levels of twin line arrays. However, the other shading schemes at frequencies other than at or near 850 Hz were all affected by the backlobe levels (see figures 10a through 12b) created at 270°.

Another expected difference between the twin line array simulations at 850 Hz was the effect caused on the sidelobe level by the increased array length. Because a larger array size results in a smaller SLL, the peak and average SLLs will be less sensitive to shading and phasing errors. This contrast can be observed by the examples shown in figures 11b and 14b. The only notable difference between figure 7 of the single line array ($N = 16, f = 850$ Hz) and figure 14 of the twin line array ($N = 62, f = 850$ Hz) on the peak SLL is with the BLAC and HAMM shading methods. However, the effects of array size on the average SLL are clearly shown regardless of shading methods used. BLAC and HAMM shading are more sensitive to random shading when applied to a twin line array.

The overall shading perturbation effects on the twin line array were very similar to the effects on the single line array. Whether the errors are from amplitude or phase, Tria shading is the best choice for low peak SLL and the least sensitive to amplitude and phase perturbations. Therefore, for the twin line array when backlobe level is minimum, TRIA shading is best suited; otherwise, any shading method other than RECT may be used. The effects of backlobe levels on the peak average SLL were much more severe than the effects of array size and amplitude or phase perturbation. So, any significant backlobe level must be nulled. Lobe nulling methods are straightforward and are documented in the context of broadband transmit array radiation pattern control in reference 1.

Case 2a considers the TLTA with $N = 30$ at $f = 750$ Hz in figures 10a and 10b; $N = 30$ at $f = 850$ Hz in figures 11a and 11b; and $N = 30$ at $f = 950$ Hz in figures 12a and 12b.

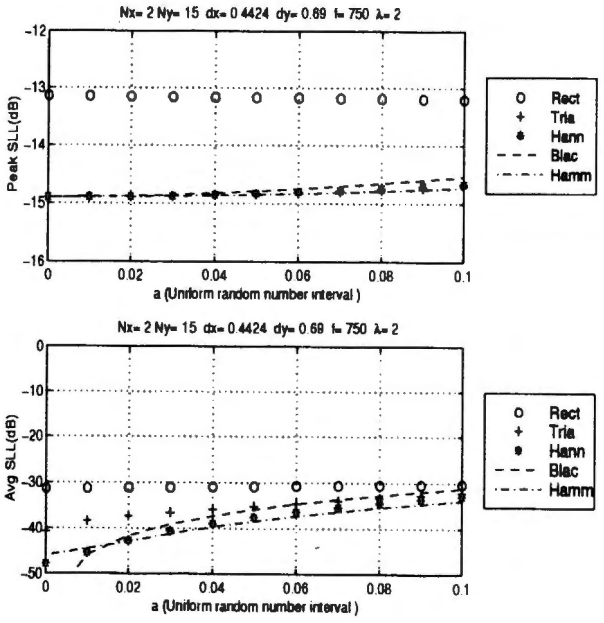

Figure 10a. Random Shading Effects on the Peak and Average SLL of Beam Patterns for N = 30, f = 750 Hz TLTA

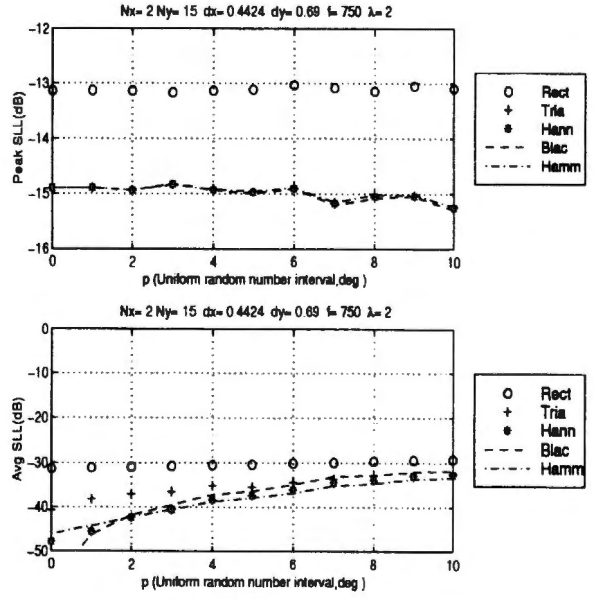

Figure 10b. Random Phasing Effects on the Peak and Average SLL of Beam Patterns for N = 30, f = 750 Hz TLTA

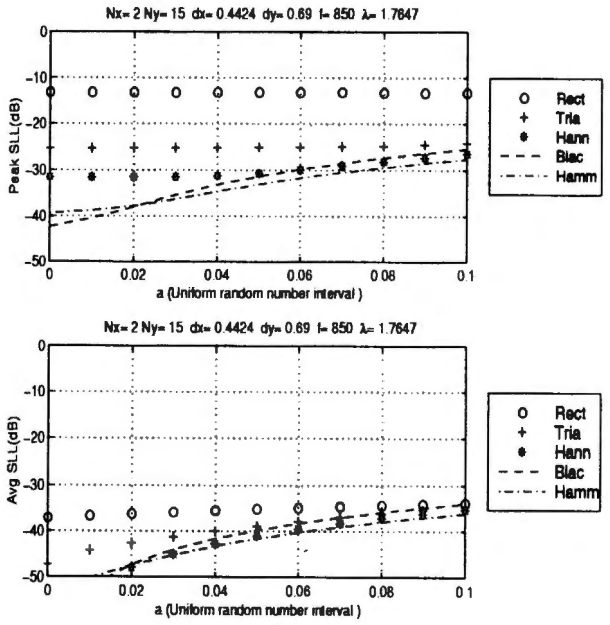

Figure 11a. Random Shading Effects on the Peak and Average SLL of Beam Patterns for N = 30, f = 850 Hz TLTA

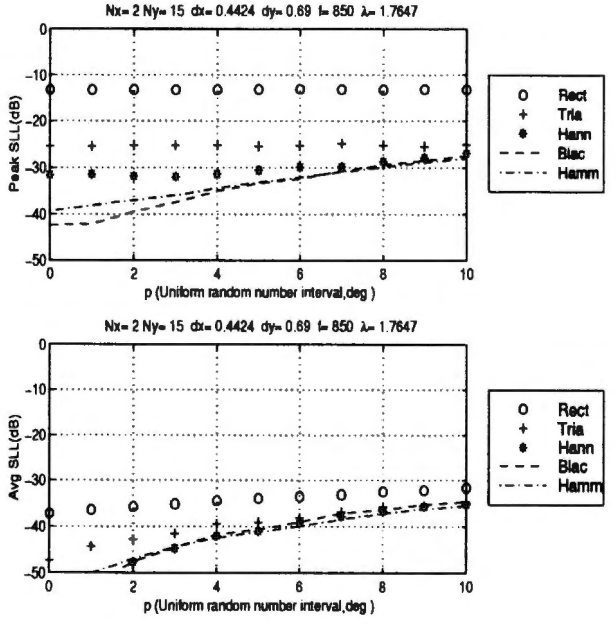

Figure 11b. Random Phasing Effects on the Peak and Average SLL of Beam Patterns for N = 30, f = 850 Hz TLTA

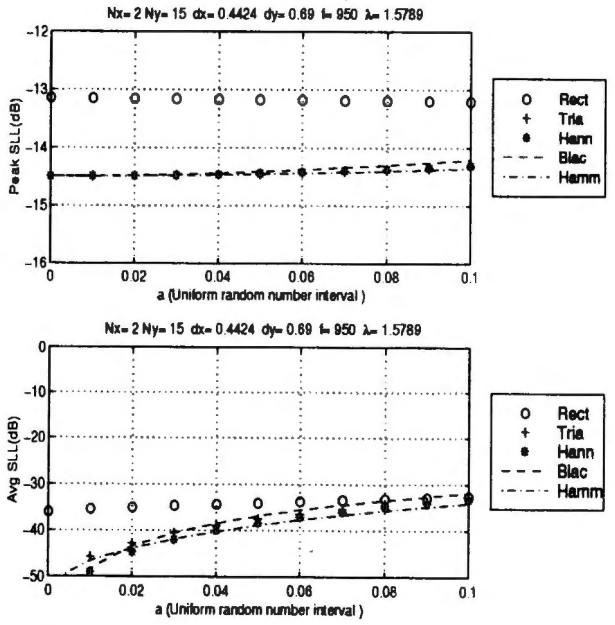

Figure 12a. Random Shading Effects on the Peak and Average SLL of Beam Patterns for N = 30, f = 950 Hz TLTA

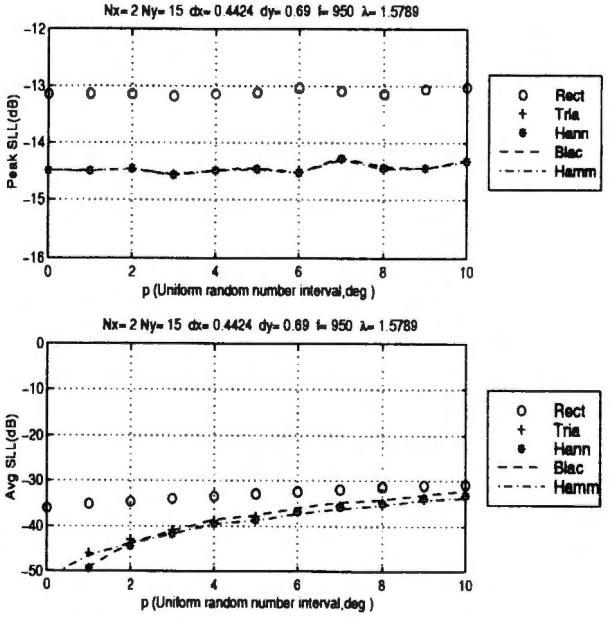

Figure 12b. Random Phasing Effects on the Peak and Average SLL of Beam Patterns for N = 30, f = 950 Hz TLTA

Case 2b considers the TLTA with $N = 62$ at $f = 750$ Hz in figures 13a and 13b; $N = 62$ at $f = 850$ Hz in figures 14a and 14b; and $N = 62$ at $f = 950$ Hz in figures 15a and 15b.

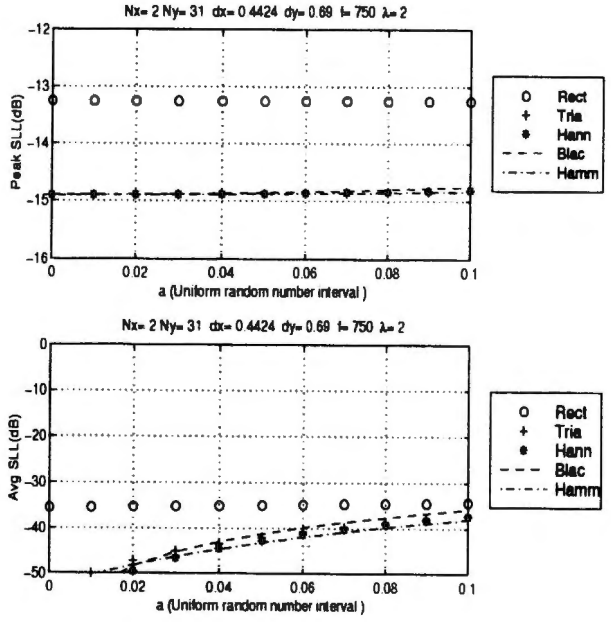

Figure 13a. Random Shading Effects on the Peak and Average SLL of Beam Patterns for N =62, f = 750 Hz TLTA

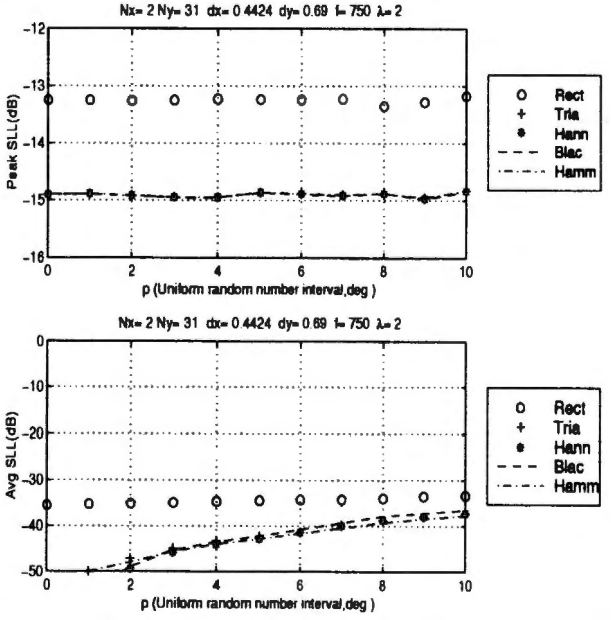

Figure 13b. Random Phasing Effects on the Peak and Average SLL of Beam Patterns for N = 62, f = 750 Hz TLTA

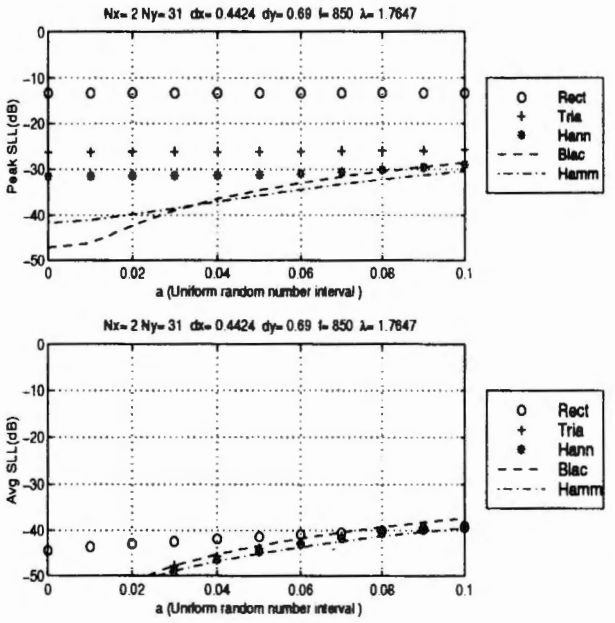

Figure 14a. Random Shading Effects on the Peak and Average SLL of Beam Patterns for N =62, f = 850 Hz TLTA

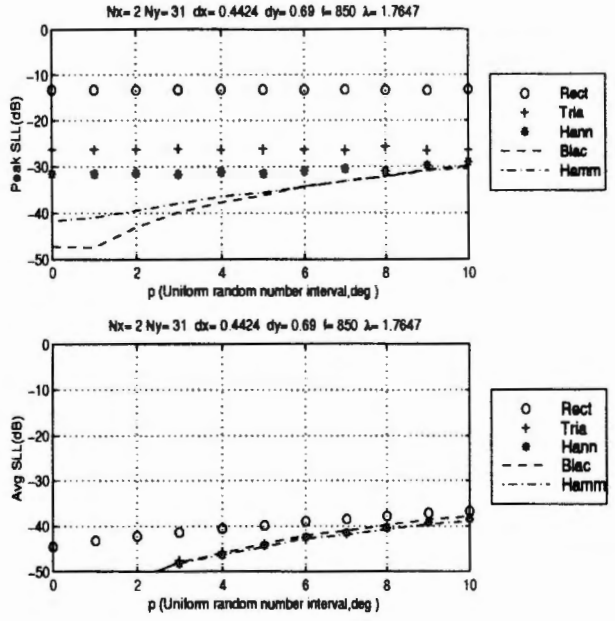

Figure 14b. Random Phasing Effects on the Peak and Average SLL of Beam Patterns for N = 62, f = 850 Hz TLTA

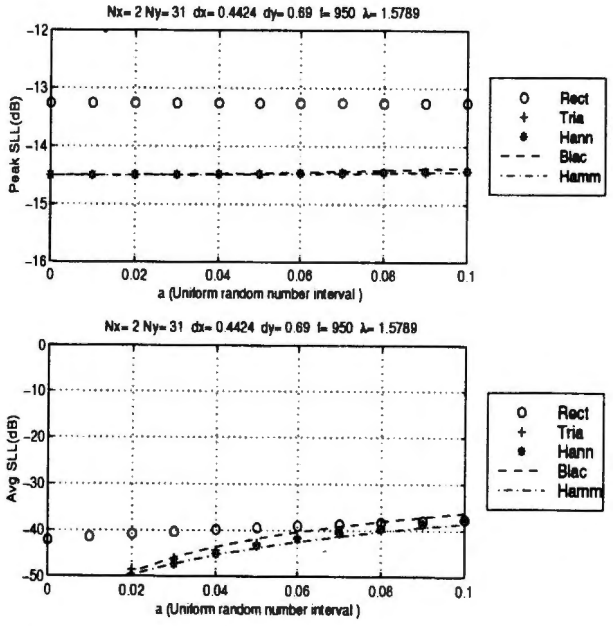

Figure 15a. Random Shading Effects on the Peak and Average SLL of Beam Patterns for N =62, f = 950 Hz TLTA

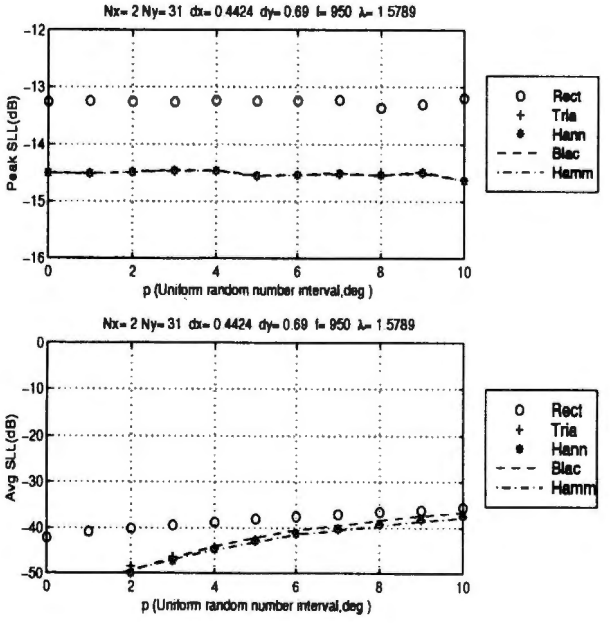

Figure 15b. Random Phasing Effects on the Peak and Average SLL of Beam Patterns for N = 62, f = 950 Hz TLTA

5. SUMMARY

The effects of amplitude and phase random perturbations on the peak and average sidelobe levels of beam patterns for single line and twin line arrays were studied. Rectangular, triangular, Hanning, Blackman, and Hamming shading schemes were compared from the standpoint of average and peak sidelobe level. Results from the single line and twin line towed arrays are very similar. When the backlobe level from the twin line array pattern is suppressed, the only notable difference is due to array size. Effects of amplitude and phase errors were less pronounced on the larger array sizes. When using the rectangular shading for the single line array, the peak and average SLLs were about -13.4 dB and less than -30 dB, respectively. BLAC shading gave the smallest peak and average SLLs. Triangular shading gave sufficiently low peak SLL (< -25 dB) and average SLL (< -35 dB) and was the least sensitive to amplitude and phase errors. Hence, triangular shading is preferred over the other shading methods (rectangular, Hanning, Blackman, and Hamming).

REFERENCES

1. N. Owsley, "Long-Range Acoustic Communications with a Multiline Towed Array Transmitter and Receiver," NUWC-NPT Technical Report 10,846, Naval Undersea Warfare Center Division, Newport, RI, 27 October 1997.

2. N. Owsley et al., *Array Signal Processing*, Prentice Hall, Englewood Cliffs, NJ, 1985.

3. R. Urick, *Principles of Underwater Sound*, McGraw-Hill, New York, 1983.

4. W. S. Burdic, *Underwater Acoustic System Analysis*, Prentice Hall, Englewood Cliffs, NJ, 1991.

DISTRIBUTION LIST

External

Naval Sea Systems Command (PEO USW ASTO - A. Hommel, J. Jones, T. Nguyen, J. Thompson, R. Zarnich)

Office of Naval Research
ONR 321 (K. Dial, C. Gaumond, N. Harned, D. Davison)
ONR 322M (A. Benson, Dr. T. Curtin)

Office of Chief of Naval Operations
N-875 (E. Joyal)

Internal

Codes:

019	R. Pikul
21	R. Martin
212	R. Garber
2122	J. Schwell
2123	C. Carter, G. Bowman, N. Owsley (10 Copies), B. Adal, R. Kneipfer
34	P. Trask
3498	C. P. Amidon
5441	Library (2 Copies)

Total: 34